The interaction between light impurities and vacancies in titanium and aluminum metals: A DFT study

Andrey I. Kartamyshev [a,*], Dat Duy Vo [b], Alexey G. Lipnitskii [a]

[a] Belgorod National Research University, 85 Pobeda St., Belgorod 308015, Russian Federation
[b] Ton Duc Thang University, 19 Nguyen Huu Tho Str., Tan Phong Ward, District 7, Ho Chi Minh City, Vietnam

Available online 30 May 2016

Abstract

In this paper, we present binding energies between hydrogen (H), carbon (C), nitrogen (N) and oxygen (O) atoms and a vacancy in the hexagonal closed-packed (HCP) lattice of titanium (Ti) and the face centered cubic (FCC) lattice of aluminum (Al), calculated using the density functional theory (DFT). We have also investigated the trapping of up to five hydrogen atoms by a vacancy and the reduction of the vacancy formation energy, due to the formation of a hydrogen–vacancy complex. We used the molecular-dynamics modeling with consecutive relaxation at $0\,K$ to obtain an atomic configuration of the vacancy–impurity complex, corresponding to the global energy minimum. According to our calculations, C–V, H–V, C–(H–V), N–(H–V) complexes are stable in the Al lattice with only H–V complex being stable in Ti. The formation of C–(H–V) and N–(H–V) complexes in the Al lattice results in the negative vacancy formation energy. The formation of H–V complex decreases the vacancy formation energy by $0.26\,eV$ in the Ti lattice. A vacancy in the Ti lattice can trap up to four hydrogen atoms.

1. Introduction

One of the outstanding implications of introducing hydrogen into metal is the possibility of increasing of the vacancy concentration in this material by several orders of magnitude, the so-called superabundant vacancy (SAV) formation. The physical kernel of this effect is a trapping of hydrogen atoms into vacancies, leading to a decrease in the vacancy formation energy.

In 1993 the SAV was first discovered experimentally by Fukai and co-workers in Pd [1] and Ni [2]. Since then the SAV has been observed in many metallic systems such as Cu [3], Ti [4], Pd and Pd alloys [5–8], Al [9], Mn [10], Fe [10,11], Mo [12], Cr [13], Co [10], Ni [14], Ni-Fe alloy [15], Nb [16–18].

In some cases, the concentration of vacancies can become as large as 10% and more [10,19,20]. One of the reasons for this behavior is the formation of different defects, e.g., voids [21] as in the case of Al [9], Ni [22], Fe [23,24], steels [25], and/or dislocation loops [26–28].

It is important to note, that H atoms may have a high number of configurations inside a vacancy,

* Corresponding author.
E-mail addresses: andrei_kart@mail.ru (A.I. Kartamyshev), duydat_bel@yahoo.com (D.D. Vo), lipnitskii@bsu.edu.ru (A.G. Lipnitskii).

leading to a higher configuration entropy of a crystal with H-vacancy complexes compared with a crystal with single vacancies and interstitial H atoms. To investigate the effects of SAV formation on material from a theoretical point of view, one has to consider the positions of hydrogen atoms inside a vacancy and the maximum number of hydrogen atoms that can be trapped by vacancy. In the aluminum lattice, it was observed that a hydrogen atom diffuses towards the lattice vacancy to occupy it [29]. Instead of occupying the lattice site from which an aluminum atom was removed during vacancy formation, the hydrogen atom locates at some asymmetrical point which is away from the vacancy's center. Lu and Kaxiras [30] suggested that, in principle, up to 12 atoms can be accommodated in a single vacancy in the Al lattice. More recently, Gunaydin, et al. [31] reported that trapping of multiple H atoms in a single vacancy in Al is possible only for extreme H loading condition, i.e., for H concentration many orders of magnitude above the solubility limit given by the equilibrium with H_2 gas at ambient conditions (10^{-9} at $300\,K$ and $1\,atm$). Instead, under H-loading conditions used in most diffusion experiments, empty vacancies would coexist with the vacancies filled by one or at most two H atoms. Reviewing the conflicting results, from Lu and Kaxiras [30] on one hand and from Gunaydin et al. [31] on the other hand, Lars Ismer, et al. studied the interactions between hydrogen impurities and vacancies in FCC Al lattice by first-principle (*ab initio*) methods but with a more critical estimation on the binding energy of the H-vacancy complex [32]. They found that a single vacancy in Al lattice can trap 10 hydrogen atoms, not 12 as reported in the work of Lu and Kaxiras [30]. The difference occurs because of the definition of the trapping energy of hydrogen impurities in vacancies of each author. However, we can see the common result in the two works that hydrogen atoms can interact with the vacancies forming H-vacancy complexes. Moreover, trapping of multiple H atoms in a single vacancy in Al lattice decreases the vacancy formation energy and this phenomenon could be related to the observed hydrogen-induced superabundant vacancy formation and vacancy clustering.

However, until now combined influence on SAV of H and other light elements such as C, O and N as well as trapping of H atoms by the monovacancy in the Ti lattice were poorly studied. At the same time the possibility of such influence is indicated by experimental data on Al lattice with C and H impurities [33]. Number of pores is increased after preliminary annealing. In this connection, in the present article, we investi-

gate combined influence of H, C, N and O atoms on the formation of their complexes with monovacancy and vacancy formation energy from first principles (*ab initio*). The investigation was performed for FCC Al and HCP Ti lattices, their alloys being widely used because of their high specific strength and corrosion resistance.

2. Calculation method

Calculations were performed in the framework of the density functional theory (DFT) [34,35] within the generalized gradient approximation (GGA) using the functional of Perdew et al. [36,37] for description of the exchange-correlation energy and the projected augmented wave (PAW) method [38] as implemented in ABINIT code [39]. Point defects were considered within supercell model. The list of point defects included an impurity atom in the interstitial site, a monovacancy and monovacancy-impurity complexes. Brillouin-zone (BZ) integrals were approximated using the special *k*-point sampling of Monkhorst and Pack [40]. Full energies of supercells were calculated after relaxation to equilibrium positions of atoms and volumes at $0\,K$. Relaxation was performed in several steps. Initial configurations included an impurity atom in the center of a monovacancy and the impurity atom in the center of interstitial site of the HCP lattice. Molecular-dynamics modeling were performed for initial configurations using Verlet algorithm [41] at $300\,K$ and consecutive cooling down to $100\,K$ using Nose–Hoover thermostat [42]. Final equilibrium configurations were determined by relaxation of supercells with the Broyden–Fletcher–Goldfarb–Shanno method [43] to the energy minimum at $0\,K$. The relaxation was stopped when all forces acting on the atoms were converged to within $2.5\,meV/Å$.

The favorable occupation site of an impurity is defined by a difference of solution energies of this impurity at different positions (ΔE_S). The solution energy is calculated by the following formula:

$$E_S^X = E[X^{T/O} + M_n] - E[M_n] - \frac{1}{2}E[X_2], \qquad (1)$$

where $E[X^{T/O} + M_n]$ are the total energies of the system with n atoms of metal M ($M =$ Ti, Al) when atom X is at tetrahedral (T) or octahedral (O) interstitial site, $E[M_n]$ is the energy of pure system with n atoms of metal M, $E[X_2]$ is the energy of molecule X_2 ($X =$ H, C, N and O) in the vacuum or in the case of carbon – the energy of graphene cell with two atoms.

In the case of vacancy-impurity system, the stability of each configuration is defined by the binding energy which was calculated by the following formula:

$$E_C^{X-V} = E[X^{T/O} + M_n] + E[V + M_{n-1}] - E[M_n]$$
$$- E[X^{T/O} - V + M_{n-1}], \qquad (2)$$

where $E[X^{T/O} + M_n]$ is the total energy of the supercell with n atoms of metal M ($M =$ Al, Ti) and the impurity X in the T/O site ($X =$ H, C, N and O), $E[M_n]$ is the total energy of the supercell with n atoms of metal, $E[V + M_{n-1}]$ is the total energy of the supercell with $(n-1)$ metal atoms and one vacancy, $E[X^{T/O} - V + M_{n-1}]$ is the total energy of the supercell with the complex X – vacancy and $(n-1)$ metal atoms. In the case of the X–(H–V) complexes V is replaced by (H–V) in this equation.

Formation vacancy energies were calculated as follows:

$$E_V^f = E[V + M_{n-1}] - \frac{n-1}{n} E[M_n] \qquad (3)$$

$$E_V^f[X] = E_V^f - E_C^{X-V} \qquad (4)$$

Here E_V^f and $E_V^f[X]$ are vacancy formation energies in pure metal and in the metal with (X–V) complexes, correspondingly. In the case of the (X–(H–V)) complexes E_C^{X-H-V} must be additionally subtracted from E_V^f.

Ismer et al. [32] suggested to determine changing of the energetic characteristics of ($V-n$H) complex (a vacancy and n atoms of hydrogen) stepwise form by adding impurity atoms one by one. Using this approach we can write the cohesive energy between a hydrogen atom and the ($V-(n-1)$H) complex as follows:

$$E(n) = E[V - (n-1)H + M_{n-1}] + E[H^O + M_n]$$
$$- E[V - nH + M_{n-1}] - E[M_n], \qquad (5)$$

where $E[V-(n-1)H+M_{n-1}]$ is the total energy of the supercell with ($V-(n-1)$H) complex, $E[V-n$H$+M_{n-1}]$ is the total energy of the supercell with ($V-n$H) complex.

3. Vacancy – impurity interactions in the aluminum lattice

The supercell contained $2 \times 2 \times 2$ cubic unit cells of the FCC aluminum lattice. The calculations were performed using an energy cutoff of $600\,\text{eV}$ for the plane-wave basis set and $2 \times 2 \times 2$ k-points grid in the Brillouin zone. Such a choice of the main parameters

Table 1
Calculated solution energies of light elements in the tetrahedral and octahedral sites in the aluminum lattice.

Atom	E_T, eV	E_O, eV
	eV	
H	0.70	0.85
C	1.31	1.25
N	−2.87	−2.00
O	−3.70	Unstable

Table 2
The binding energies between impurity atoms and vacancies (V) or hydrogen–vacancy complexes (H–V) in the aluminum lattice.

Interaction	E_b, eV
H–V	0.39
C–V	0.18
N–V	−0.69
O–V	0.02
C– (H–V)	0.77
N–(H–V)	0.56
O–(H–V)	−0.07

ensures an energy convergence to $1\,\text{meV/atom}$. The solution energies of C, N, O and H atoms in the tetrahedral and octahedral sites calculated by Eq. (1) are shown in Table 1.

Solution energies for H atoms are consistent with the known experimental data (from 0.65 to $0.71\,\text{eV}$) [44–47]. We found O atom moving from octahedral to tetrahedral interstitials sites during simulation and so the corresponding solution energy was not calculated.

Energetic properties of the impurity–vacancy complexes in the aluminum lattice calculated by Eq. (2) are shown in Table 2.

The calculated binding energy E_C^{H-V} between a hydrogen atom and a vacancy is close to the experimental value of $0.43\,\text{eV}$ [48]. The negative binding energy for the N–V complex means that there is a repulsive interaction between them and a nitrogen atom is not responsible for an increase in the vacancy concentration. However, in the presence of a hydrogen atom the binding energy becomes positive and the formation of (N–(H–V)) complex is energetically favorable. The calculated N–H bond length of $1.04\,\text{Å}$ in the (N–(H–V)) complexes is close to the experimental data of 1.01–$1.03\,\text{Å}$ [49]. A considerable increase in the binding energy was found for (C–(H–V)) complex in contrast to the (C–V) one.

The vacancy formation energies in pure aluminum and those in the presence of impurities calculated by Eqs. (3) and (4) are listed in Table 3.

Table 3
Vacancy formation energies in the aluminum lattice with impurities and in the pure one.

Impurity	$E_v{}^f$, eV
C	0.37
H	0.16
H, C	−0.61
H, N	−0.40
0 (pure)	0.55

Table 4
The binding energies between an impurity atom and a vacancy (V) in the titanium lattice.

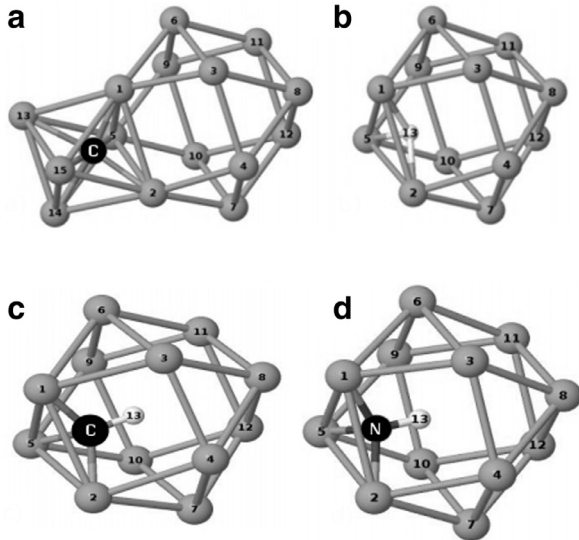| Interaction	E_b, eV
H–V	0.26
C–V	−0.84
N–V	−1.72
O–V	−1.15

Fig. 1. The configurations of the vacancy-impurity complexes C–V (*a*), H–V (*b*), C–(H–V) (*c*), N–(H–V) (*d*) in the aluminum lattice. H atoms are shown by white balls; C, N atoms are black ones; 12 Al atoms form the 1st coordination sphere around the vacancy (V) site of the lattice.

We can see from Table 3 that the vacancy formation energy values reduce from 0.55 eV in the pure aluminum to 0.37 eV in the presence of the vacancy–carbon complex and to 0.16 eV in the presence of the vacancy–hydrogen one. This explains an increase in the vacancy concentration in aluminum with hydrogen and carbon impurities [33]. Moreover, formations of the (C– (H–V)) and the (N–(H–V)) complexes result in the negative vacancy formation energies.

These vacancies are no longer thermally activated and new free vacancies are formed in order to keep the equilibrium concentration of the free vacancies. This mechanism can explain SAV formation in the aluminum lattice at the presence of both C and H impurities as reported in paper [33]. Configurations of stable complexes of the point defects are shown in Fig. 1.

4. Vacancy – impurity interactions in the titanium lattice

The supercell contained $3 \times 3 \times 2$ unit cells of the HCP titanium lattice. The calculations were performed using an energy cutoff of 600 eV for the plane-wave basis set and $4 \times 4 \times 4$ *k*-points grid in the Brillouin zone. Such a choice of the main parameters ensures energy convergence to 1 meV/atom.

In the case of a hydrogen atom

$$\Delta E_S = 0.06 \, eV \left(\Delta E_S = E_S{}^X(tet.) - E_S{}^X(\text{oct.}) \right).$$

This value is in good agreement with the results of other DFT calculations being equal to 0.01 eV [50] and 0.12 eV [51]. Carbon, nitrogen and oxygen atoms also occupy octahedral interstitial sites with values of ΔE_S equal to 2.13, 1.70, and 1.16 eV correspondingly. We can see that the solution energy for hydrogen is less than the corresponding value for other impurities by the order of magnitude. Hence, we can expect a higher cohesive energy of a hydrogen atom with crystal defects (including vacancies) in comparison with that of carbon, nitrogen and oxygen atoms.

The energy properties of the impurity – vacancy complexes in the titanium lattice calculated by Eq. (2) are shown in Table 4.

As we can see from Table 4, the H–V complex only has positive binding energy, whereas other impurity – vacancy complexes being unstable. The negative binding energy between other impurities and vacancy shows that there will be repulsive interaction between them. The configuration of H–V complex in the Ti lattice is presented in Fig. 2.

From our calculations by Eq. (3) $E_v{}^f = 2.12$ eV. Difference between this value and other DFT calculations [52] is less than 1%. Using Eq. (4) we found that the formation of complex $H–V$ reduces the vacancy formation energy by 0.26 eV. It is considerably higher than the average kinetic energy of atoms ~$3/2k_BT = 0.039$ eV at 300 K.

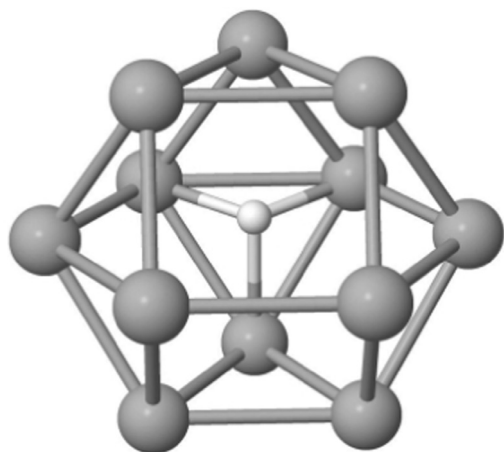The binding energies E_b calculated by Eq. (5) for the titanium lattice are presented in Table 5.

Fig. 2. Configuration of the H–*V* complex in the Ti lattice.
H atom is shown by a white ball; 12 Ti atoms form the 1st coordination sphere around the vacancy (*V*) site of the lattice.

Table 5
The *n*-dependence of binding energies between a hydrogen atom and the *V* − (*n* − 1)H complex.

n	E_b, eV
2	0.25
3	0.38
4	0.08
5	−0.05

We can conclude from Table 5 that the maximum number of hydrogen atoms that can be trapped by a monovacancy in HCP titanium lattice is four. Earlier DFT calculations [51] have shown that a monovacancy in HCP titanium lattice can contain up to three these atoms. The difference between our calculations and those of Ref. [51] is explained by the simplified relaxation of initial atomic configurations of complexes used in Ref. [51] that led to a configuration in the local energy minimum. Using molecular-dynamics modeling before relaxation at 0 K we obtained more energetically favorable atomic configurations with number of hydrogen atoms more than three. Trapping of hydrogen atoms by vacancies can lead to reduction of the vacancy formation energy and consequently to an increase in the vacancy concentration by several orders of magnitude as was found by Fukai in the nickel lattice for the first time [2].

5. Conclusions

Using density functional theory calculations, we investigated the interactions of the impurity atoms of hydrogen, carbon, nitrogen and oxygen with monovacancies in the HCP titanium and FCC aluminum lattices. The results of this work can be summarized as follows:

1. Impurities such as hydrogen, carbon, nitrogen and oxygen atoms occupy octahedral interstitial sites in both Al and Ti lattices except for hydrogen and oxygen atoms in the Al that occupy tetrahedral sites.
2. The C–*V*, H–*V*, C–(H–*V*), and N–(H–*V*) complexes are stable in the Al lattice. Except for the H–*V* complex with positive cohesive energy, other impurity–vacancy complexes are unstable in the Ti lattice.
3. The formation of C–(H–*V*) and N–(H–*V*) complexes in Al results in the negative vacancy formation energy. The formation of H–*V* complex in the HCP titanium lattice decrease the vacancy formation energy by 0.26 eV. This leads to an increase in the vacancy concentration and can result in the pore formation at the presence of corresponding impurities.
4. According to our calculations the maximum number of hydrogen atoms that can be trapped by a monovacancy in the HCP Ti lattice is four.

References

[1] Y. Fukai, N. Ōkuma, Formation of superabundant vacancies in Pd hydride under high hydrogen pressures, Phys. Rev. Lett. 73 (12) (1994) 1640–1643.

[2] Y. Fukai, N. Ōkuma, Evidence of copious vacancy formation in Ni and Pd under a high hydrogen pressure, Jpn. J. Appl. Phys. 32 (1993) L1256–L1259 Part 2. No. 9A (1993).

[3] Y. Fukai, M. Mizutani, S. Yokota, et al., Superabundant vacancy–hydrogen clusters in electrodeposited Ni and Cu, J. Alloys Compd. 2003 356–357 (2003) 270–273.

[4] D.O. Poletaev, D.A. Aksyonov, D.D. Vo, et al., Hydrogen solubility in hcp titanium with the account of vacancy complexes and hydrides: A DFT study, Comput. Mater. Sci. 114 (2016) 199–208.

[5] dos D. Santos, S. Miraglia, D. Fruchart, A high pressure investigation of Pd and the Pd–H system, J. Alloys Compd. 291 (1-2) (1999) L1–L5.

[6] Y. Fukai, Y. Ishii, Y. Goto, et al., Formation of superabundant vacancies in Pd–H alloys, J. Alloys Compd. 313 (1-2) (2000) 121–132.

[7] K. Watanabe, N. Ōkuma, Y. Fukai, et al., Superabundant vacancies and enhanced diffusion in Pd-Rh alloys under high hydrogen pressures, Scr. Mater. 1996 34 (4) (1996) 551–557.

[8] K. Sakaki, R. Date, M. Mizuno, et al., The effect of hydrogenated phase transformation on hydrogen-related vacancy formation in $Pd_{1-x}Ag_x$ alloy, Acta Mater. 54 (17) (2006) 4641–4645.

[9] H.K. Birnbaum, C. Buckley, F. Zeides, et al., Hydrogen in aluminum, J. Alloys Compd. 253 –254 (1997) 260–264.

[10] Y. Fukai, T. Haraguchi, E. Hayashi, et al., Hydrogen-induced superabundant vacancies and diffusion enhancement in some FCC metals, Defect Diffus. Forum. 194 –199 (2001) 1063–1068.

[11] Y. Fukai, K. Mori, H. Shinomiya, The phase diagram and superabundant vacancy formation in Fe–H alloys under high hydrogen pressures, J. Alloys Compd. 348 (1-2) (2003) 105–109.

[12] Y. Fukai, Y. Kurokawa, H. Hiraoka, Superabundant vacancy formation and its consequences in metal-hydrogen alloys, J. Japan Inst. Met. Mater. 61 (8) (1997) 663–670.

[13] Y. Fukai, M. Mizutani, Phase diagram and superabundant vacancy formation in Cr-H alloys, Mater. Trans., JIM. 43 (5) (2002) 1079–1084.

[14] Y. Fukai, Y. Shizuku, Y. Kurokawa, Superabundant vacancy formation in Ni–H alloys, J. Alloys Compd. 329 (1-2) (2001) 195–201.

[15] Y. Fukai, T. Hiroi, N. Mukaibo, et al., Formation of hydrogen-induced superabundant vacancies in electroplated nickel–iron alloy films, J. Japan Inst. Met. Mater. 71 (4) (2007) 388–394.

[16] H. Koike, Y. Shizuku, A. Yazaki, et al., Superabundant vacancy formation in Nb–H alloys; resistometric studies, J. Phys. Condens. Matter. 16 (8) (2004) 1335–1349.

[17] T. Iida, Y. Yamazaki, T. Kobayashi, et al., Enhanced diffusion of Nb in Nb–H alloys by hydrogen-induced vacancies, Acta Mater 53 (10) (2005) 3083–3089.

[18] J. Čížek, I. Procházka, F. Bečvář, et al., Hydrogen-induced defects in bulk niobium, Phys. Rev. B. 69 (22) (2004) 224106.

[19] Y. Fukai, Formation of superabundant vacancies in M–H alloys and some of its consequences: a review, J. Alloys Compd. 2003 356 –357 (2003) 263–269.

[20] Y. Fukai, Superabundant vacancies formed in metal-hydrogen alloys, Phys. Scr. T103 (1) (2003) 11.

[21] A.M. Cuitiño, M. Ortiz, Ductile fracture by vacancy condensation in f.c.c. single crystals, Acta Mater. 44 (2) (1996) 427–436.

[22] H. Osono, T. Kino, Y. Kurokawa, et al., Agglomeration of hydrogen-induced vacancies in nickel, J. Alloys Compd. 231 (1-2) (1995) 41–45.

[23] I.M. Bernstein, Hydrogen-induced cracking in iron: Morphology and crack path dependence, Metall. Trans. 1 (11) (1970) 3143–3150.

[24] B.B. Rath, I.M. Bernstein, The relation between grain-boundary orientation and intergranular cracking, Metall. Trans. 2 (10) (1971) 2845–2851.

[25] Q.-Z. Chen, W. Chu, Y. Wang, et al., *In situ* tem observations of nucleation and bluntness of nanocracks in thin crystals of 310 stainless steel, Acta Metall. Mater. 43 (12) (1995) 4371–4376.

[26] Y. Fukai, Formation of superabundant vacancies in metal hydrides at high temperatures, J. Alloys Compd. 231 (1-2) (1995) 35–40.

[27] V.G. Gavriljuk, V. Bugaev, Y. Petrov, et al., Hydrogen-induced equilibrium vacancies in FCC iron-base alloys, Scr. Mater. 34 (6) (1996) 903–907.

[28] T.B. Flanagan, J. Clewley, H. Noh, et al., Hydrogen-induced lattice migration in Pd–Pt alloys, Acta Mater 46 (6) (1998) 2173–2183.

[29] B.E.F. Constance, B.K. Rao, Position of hydrogen atom in a vacancy in aluminum metal – an AB initio study, Rev. Adv. Mater. Sci. 5 (1) (2003) 17–23.

[30] G. Lu, E. Kaxiras, Hydrogen embrittlement of aluminum: the crucial role of vacancies, Phys. Rev. Lett. 94 (15) (2005) 155501.

[31] H. Gunaydin, S. Barabash, K. Houk, et al., First-principles theory of hydrogen diffusion in aluminum, Phys. Rev. Lett. 101 (7) (2008) 075901.

[32] L. Ismer, M. Park, A. Janotti, et al., Interactions between hydrogen impurities and vacancies in Mg and Al: A comparative analysis based on density functional theory, Phys. Rev. B. 80 (18) (2009) 184110.

[33] Y. Shimomura, I. Mukuoda, Q. Chen, et al., Impurity atoms responsible for the void formation in quenched pure aluminum, Mater. Trans., JIM. 36 (3) (1995) 413–419.

[34] P. Hohenberg, W. Kohn, Inhomogeneous electron gas, Phys. Rev. B. 136 (3) (1964) 864–871.

[35] W. Kohn, L.J. Sham, Self-consistent equations including exchange and correlation effects, Phys. Rev. A. 140 (4) (1965) 1133–1138.

[36] J.P. Perdew, K. Burke, Y. Wang, Generalized gradient approximation for the exchange-correlation hole of a many-electron system, Phys. Rev. B. 1996 54 (23) (1996) 16533–16539.

[37] J.P. Perdew, K. Burke, M. Ernzerhof, Generalized gradient approximation made simple, Phys. Rev. Lett. 77 (18) (1996) 3865–3868.

[38] P.E. Blöchl, Projector augmented-wave method, Phys. Rev. B. 1994 50 (24) (1994) 17953–17979.

[39] X. Gonze, J. Beuken, R. Caracas, et al., First-principles computation of material properties: the ABINIT software project, Comput. Mater. Sci. 25 (3) (2002) 478–492.

[40] H.J. Monkhorst, J.D. Pack, Special points for Brillouin–zone integrations, Phys. Rev. B. 13 (12) (1976) 5188–5192.

[41] L. Verlet, Computer "experiments" on classical fluids. I. Thermodynamical properties of Lennard-Jones molecules, Phys. Rev. 159 (1) (1967) 98–103.

[42] D.J. Evans, B.L. Holian, The Nose–Hoover thermostat, J. Chem. Phys. 83 (8) (1985) 4069.

[43] J.D. Head, M.C. Zerner, A Broyden—Fletcher—Goldfarb—Shanno optimization procedure for molecular geometries, Chem. Phys. Lett. 122 (3) (1985) 264–270.

[44] R.A.H Edwards, W. Eichenauer, Reversible hydrogen trapping at grain boundaries in superpure aluminium, Scr. Metall. 14 (9) (1980) 971–973.

[45] W. Eichenauer, K. Hattenbach, A. Pebler, The solubility of hydrogen in solid and liquid aluminum, Zeitschrift Für Met 52 (1961) 682–684.

[46] H. Sugimoto, Y. Fukai, Solubility of hydrogen in metals under high hydrogen pressures: Thermodynamic calculations, Acta Metall. Mater. 40 (9) (1992) 2327–2336.

[47] M. Ichimura, H. Katsuta, Y. Sasajima, et al., Hydrogen and deuterium solubility in aluminum with voids, J. Phys. Chem. Solids. 49 (10) (1988) 1259–1267.

[48] S. Linderoth, Hydrogen diffusivity in aluminium, Philos. Mag. Lett. 57 (4) (1988) 229–234.

[49] X. Zhao, J. Sudmeier, W. Bachovchin, et al., Measurement of NH bond lengths by fast magic-angle spinning solid-state NMR spectroscopy: a new method for the quantification of hydrogen bonds, J. Am. Chem. Soc. 123 (44) (2001) 11097–11098.

[50] J.H. Dai, Y. Song, R. Yang, Influence of impurities on phase stability of martensites in titanium, Philos. Mag. 92 (18) (2012) 2272–2285.

[51] D. Connétable, J. Huez, É. Anrieu, et al., First-principles study of diffusion and interactions of vacancies and hydrogen in hcp-titanium, J. Phys. Condens. Matter. 23 (40) (2011) 405401.

[52] G. Vérité, F. Willaime, C.C. Fu, Anisotropy of the vacancy migration in Ti, Zr and Hf hexagonal close-packed metals from first principles, Solid State Phenom 129 (2007) 75–81.